iScience

Article

Bitter taste receptor T2R14-Gαi coupling mediates innate immune responses to microbial quorum sensing molecules in cystic fibrosis

Graphical abstract

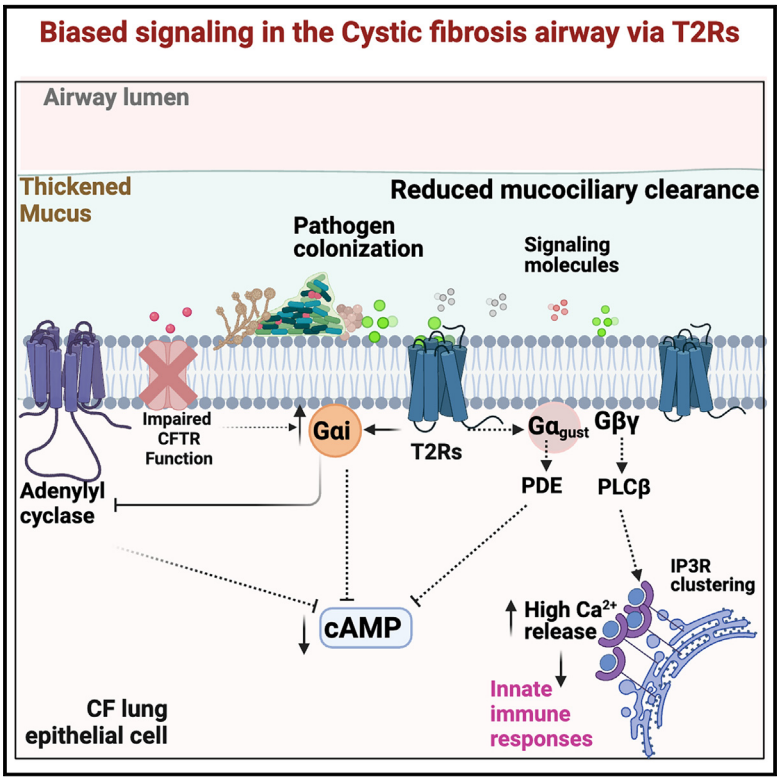

Highlights

- Gαi-T2R14 coupling is important for immune responses in CF airway mucosa
- Gαi is upregulated in CF airway epithelial cells
- T2R14 detects quorum sensing molecules and triggers intracellular calcium signaling
- T2R14 activation enhances the innate immune response to live bacteria in CF airway cells

Authors

Nisha Singh, Ryan H. Cunnington, Anjali Bhagirath, ..., Shyamala Dakshisnamurti, John W. Hanrahan, Prashen Chelikani

Correspondence

prashen.chelikani@umanitoba.ca

In brief

Pathophysiology; Immunology; Microbiology

Singh et al., 2024, iScience 27, 111286
December 20, 2024
https://doi.org/10.1016/j.isci.2024.111286

CellPress

iScience

CellPress
OPEN ACCESS

Article

Bitter taste receptor T2R14-Gαi coupling mediates innate immune responses to microbial quorum sensing molecules in cystic fibrosis

Nisha Singh,[1,2,3] Ryan H. Cunnington,[1,2,3,9] Anjali Bhagirath,[1,2,3,8,9] Ankita Vaishampayan,[1,2,3] Mohd Wasif Khan,[1,3,4] Tejas Gupte,[1,2,3] Kangmin Duan,[1,2,3] Abdelilah S. Gounni,[3,5] Shyamala Dakshisnamurti,[1,3,6] John W. Hanrahan,[7] and Prashen Chelikani[1,2,3,4,6,10,*]

[1]Manitoba Chemosensory Biology (MCSB) research group, Rady Faculty of Health Sciences, University of Manitoba, Winnipeg, MB, Canada
[2]Department of Oral Biology, Rady Faculty of Health Sciences, University of Manitoba, Winnipeg, MB, Canada
[3]Children's Hospital Research Institute of Manitoba, Winnipeg, MB, Canada
[4]Department of Biochemistry and Medical Genetics, Rady Faculty of Health Sciences, University of Manitoba, Winnipeg, MB, Canada
[5]Department of Immunology, Rady Faculty of Health Sciences, University of Manitoba, Winnipeg, MB, Canada
[6]Department of Physiology and Pathophysiology, Rady Faculty of Health Sciences, University of Manitoba, Winnipeg, MB, Canada
[7]Department of Physiology, McGill University, Montréal, QC, Canada
[8]Dalhousie University, Faculty of Dentistry, Halifax, NS, Canada
[9]These authors contributed equally
[10]Lead contact
*Correspondence: prashen.chelikani@umanitoba.ca
https://doi.org/10.1016/j.isci.2024.111286

SUMMARY

Cystic fibrosis (CF) is an autosomal recessive disease characterized by microbial infection and progressive decline in lung function, leading to significant morbidity and mortality. The bitter taste receptor T2R14 is a chemosensory receptor that is significantly expressed in airways. Using a combination of cell-based assays and T2R14 knockdown in bronchial epithelial cells from CF and non-CF individuals, we observed that T2R14 plays a crucial role in the detection of bacterial and fungal signals and enhances host innate immune responses. Expression of Gαi protein is enhanced in CF bronchial epithelial cells and T2R14-Gαi specific signaling leads to increased calcium mobilization. Knockdown of T2R14 leads to reduced innate immune activation by bacterial strains deficient in quorum sensing. The results demonstrate that T2R14 helps protect against microbial infection and thus may play an important role in the innate immune defense of the CF airway epithelium.

INTRODUCTION

Cystic fibrosis (CF) is an autosomal recessive disease caused by about 700 mutations in the *cftr* gene that encodes the cystic fibrosis transmembrane conductance regulator (CFTR). It is estimated to affect approximately 75,000 people in North America, Australia, and Europe.[1] Mutations in CFTR result in the production of abnormal mucus, impaired ciliary movement, and compromised mucociliary clearance, all of which increase susceptibility to respiratory pathogens, especially *Staphylococcus aureus*, *Pseudomonas aeruginosa*, *Aspergillus fumigatus*, and *Candida* sp.[2,3] These pathogens can persist in the lungs for extended periods, manipulating or commandeering host immune responses and contributing to the decline in lung function that may ultimately prove fatal in people with CF (pwCF).

Bacterial and fungal species secrete quorum sensing molecules (QSMs) which promote biofilm formation.[4,5] QSMs include acyl-homoserine lactones (AHLs) produced by Gram-negative bacteria and autoinducer peptides (AIPs) produced by Gram-positive species. Host detection of microbial pathogens through pattern associated molecular patterns (PAMPs) by the Toll-like receptors (TLRs) has been studied extensively and shown to stimulate various innate antimicrobial responses.[6–10] However, more recent evidence indicates that chemosensory bitter taste receptors (T2Rs) that are expressed in airway epithelial cells are also able to recognize bacterial QSMs and respond by activating innate immune responses.[11–13] Bitter taste receptor 14 (T2R14) is one of the abundantly expressed chemosensory receptors in airway epithelial cells which has been linked to host-QSM detection.[14,15] The interaction of fungal QSMs (e.g., farnesol and tyrosol) with T2Rs has not yet been shown. These two QSMs are produced by various *Candida* species and often have opposing effects on fungal physiology. Farnesol can inhibit hypha and biofilm formation, whereas tyrosol promotes both.[16,17] These compounds may also have beneficial effects in the host. For example, farnesol acts on the intestinal barrier to promote its integrity[18] while tyrosol inhibits mixed species biofilms.[19] Farnesol may influence immune activation in macrophage and monocytes,[20] however the effect of tyrosol on innate immune function remains uncertain.

There is a growing body of evidence that T2Rs may act in parallel with TLRs as Pattern Recognition Receptors (PRRs). Canonical T2Rs signal through a G-protein pathway in which the binding of a bitter agonist triggers activation of gustducin ($G\alpha_{gust}$ subunit)[21] and release of $G\beta\gamma$ dimer. Gustducin stimulates phosphodiesterase to degrade cAMP,[22] while the $G\beta\gamma$ dimer promotes calcium release through the PLCβ-IP_3-IP_3R pathway. Previous studies suggest that T2R stimulation is associated with the Gαi pathway.[23–25]

Identifying the host cell receptors that interact with both bacterial and fungal signals is essential for understanding host defense and identifying potential therapeutic targets. Given the potential of T2Rs to modulate immune responses in a variety of diseases, this study examined the hypothesis that T2R14 in airway epithelial cells detect bacterial and fungal signals and mediate innate immune responses through the Gαi pathway in the CF lung.

RESULTS

T2R14 detects both bacterial and fungal signals in CF human bronchial epithelial (HBE) cells amplifying calcium mobilization by QSMs

T2R14 is a prominently expressed chemosensory bitter taste receptor in airway epithelial cells.[14,26,27] In this study, primary HBE cells from both CF (BCF) and non-CF (BD) donors, and the immortalized HBE cell lines from CF (CuFi-1) and non-CF (NuLi-1, BEAS-2B) were evaluated for TAS2R14 expression using qPCR and western blot analysis. Results indicated significantly higher TAS2R14 mRNA expression in BCF compared to BD cells (Figure 1A). Our previous nCounter analysis had revealed expression of TAS2R14 in NuLi-1 and CuFi-1 cells, with no detectable difference in expression.[14] However, differences in mRNA expression did not alter protein levels significantly (Figures 1B and 1C). As similar expression patterns were observed between non-CF cell lines NuLi-1 and BEAS-2B (data not shown), unless mentioned the experiments were pursued further in NuLi-1 cells. The expressed T2R14 was functional as demonstrated by a concentration-dependent increase in Ca^{2+} mobilization upon stimulation with the T2R14 agonist diphenhydramine or DPH, 31.5 μM to 2 mM (Figure 1D). All the cell types investigated had an EC_{50}~500 μM. This further confirmed that agonist-stimulation of T2R14 results in Ca^{2+} mobilization in HBE cells. Having detected the presence of T2R14, we employed shRNA-mediated knockdown (KD) to query the involvement of T2R14 in detecting bacterial and fungal QSMs. BD and BCF cells infected with lentivirus encoding T2R14-shRNA exhibited 70% reduction in T2R14 mRNA compared to either uninfected cells or corresponding cells infected with a scrambled shRNA as determined by qPCR (Figure 1E). Hereafter, the cells infected with lentivirus encoding T2R14-shRNA are labeled by the suffix 'T2R14 KD', and the cells infected with lentivirus encoding the scrambled shRNA are indicated by the suffix 'Sc shRNA'. Normal barrier function was maintained in air liquid interface (ALI) cultures derived from T2R14 KD - BD and BCF cells (See Figure S1). T2R14 KD - BD and BCF cells exhibited a reduction in Ca^{2+} mobilization in response to stimulation with the T2R14 agonist DPH (500 μM) (Figure 1F), consistent with decrease in T2R14 mRNA.

Next, calcium release was measured in Sc shRNA or T2R14 KD – BD and BCF cells treated with different concentrations of CF-relevant bacterial QSMs 3-oxo-12-AHL (C12, 4.5–300 μM) (*P. aeruginosa*) and Autoinducer peptide-1 (AIP-1, 50 μM) (*S. aureus*), the fungal QSMs tyrosol (15 μM–1000 μM) and farnesol (7.5 μM–500 μM) (*Candida* sp). Concentration dependent intracellular calcium mobilization was observed in response to C12 and tyrosol with an effective concentration EC_{50}, around 100 μM and farnesol (EC_{50} around 120 μM) in both BCF and BD cells (Figure 1G(i-iii)). Further, to show the specificity of T2R14 to fungal QSM farnesol and tyrosol and bacterial QSM C12, BD and BCF T2R14 KD cells were used to measure the intracellular calcium mobilization in these HBEs. Result suggested there was a T2R14 dependent significant ($^*p < 0.05$ and $^{**}p < 0.01$) decrease in calcium mobilization in these KD cells which was evident by changes in their intracellular maximal calcium mobilization responses (E_{max}) (Figure 1G(i-iii)). The Autoinducer peptide-1 (AIP-1, 50 μM) (*S. aureus*) also induces increase in intracellular calcium release (Figure 1G(iv)). This suggests that T2R14 detects not just bacterial, but also fungal QSMs and responds by eliciting a Ca^{2+} mobilization response. Next, to support our finding, HEK293T cells overexpressing T2R14 showed a concentration dependent increase in intracellular calcium mobilization upon treatments with bacterial QSM C12 and fungal QSMs farnesol and tyrosol (See Figures S2A–S2C). Overall, our finding indicates that C12, farnesol and tyrosol induced intracellular calcium responses are predominantly mediated through T2R14 in BD and BCF HBEs. We observed a higher basal response in case of C12 treatment (See Figure S2A). This could be due to non-specific response of solvent used for the preparation of C12 compound. However, we observed the EC_{50} around 60 μM in HEK 293T cells overexpressing T2R14.

T2R14-Gαi specific signaling in non-CF and CF HBEs

T2Rs are known to couple with different G-protein subunits in extraoral tissues. Hence, we profiled the expression of Gα subunits (Gαgust, Gαi, Gαs) in CF and non-CF HBEs. Western blot analysis revealed a notable upregulation of Gαi protein in CuFi-1 and BCF cells, while the levels of other Gα subunits did not vary significantly between CF and non-CF conditions (Figure 2A). As adenylyl cyclase (AC) activity is modulated by both the stimulatory Gαs and the inhibitory Gαi, an increased expression of Gαi without a concurrent change in Gαs, could intensify inhibitory signaling and reduce cAMP synthesis. Our data shows elevated Gαi expression in CF cells (CuFi-1 and BCF) compared to non-CF cells (NuLi-1 and BD) with no alterations in Gαs expression (Figures 2A and 2B and densitometry See Figure S3A). The functional relevance of enhanced Gαi protein was determined by measuring AC activity (cAMP), in the presence or absence of Gαi-specific peptide inhibitor TAT-GPR.[28] CuFi-1 cells stimulated with forskolin had lesser cAMP than NuLi-1 cells, indicating greater AC inhibition in the CF cells and correlating with enhanced Gαi in CF cells (Figure 2C). Upon blocking Gαi with the TAT-GPR peptide (100 nM for 15 min), CuFi-1 cells showed a dramatic increase in cAMP levels in response to forskolin, however no significant change was detected in NuLi-1, further emphasizing a functional role for the elevated Gαi in CF conditions.

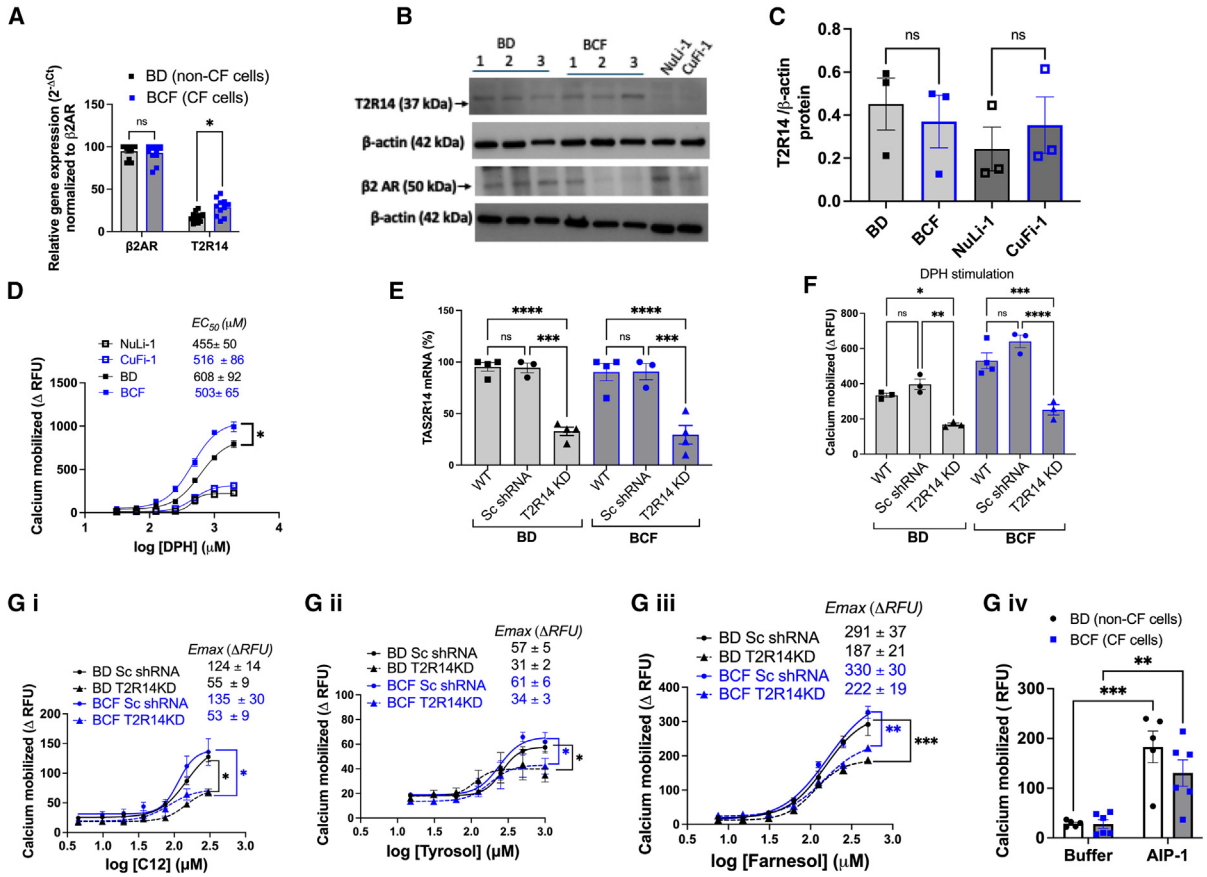

Figure 1. T2R14 detects both bacterial and fungal signals

(A) mRNA expression of T2R14 and β2-AR. Analysis of the TAS2R14 and β2-AR transcripts by qPCR on primary human bronchial epithelial cells (HBEs) BD (non-CF) and BCF (CF) (1st passage) from adult donors (three from each category). Bar graph represents average data points from three donors ($n = 3$).

(B) Representative Western blot analysis for T2R14, β2-AR and β-actin as a loading control from BD (non-CF), BCF (CF) primary HBEs from three donors, and NuLi-1 (non-CF) and CuFi-1 (CF)-hTert-immortalized HBEs.

(C) Densitometric analysis showing T2R14 expression in BD, BCF, NuLi-1 and CuFi-1 cells.

(D) Intracellular calcium mobilization using the T2R14 specific agonist diphenhydramine (DPH, 31.5 μM to 2 mM) in CF (blue symbols and lines) and non-CF cells (black symbols and lines) HBEs. The data represent SEM of at least three independent experiments performed in triplicate.

(E) shRNA-mediated knockdown (KD) of T2R14 in primary HBEs from non-CF (BD, black symbols and outline) and CF (BCF, blue symbols and outline) primary HBEs. Cells were either untransfected (WT, square symbol), or transfected with lentiviral particles containing either scramble shRNA (Sc shRNA, non-targeting control, circles) or T2R14 shRNA (T2R14 KD, triangle). Effect of shRNA on T2R14 mRNA was analyzed by qPCR.

(F) Calcium mobilization in BD, BCF either untransfected (WT) or transfected with the indicated shRNA (Sc/T2R14). Cells were treated with T2R14 specific agonist DPH. (*$p < 0.05$, **$p < 0.01$, ***$p < 0.001$, ****$p < 0.0001$). Bar graph data are SEM from $n \geq 3$ experiments.

(G) (i–iii) Effect of C12, tyrosol and farnesol on calcium mobilization in BD, BCF Sc shRNA and T2R14 KD HBEs. Intracellular calcium release in BD and BCF cells was measured following treatment with C12 (4.5 μM–300 μM), tyrosol (7.5 μM–1000 μM) and farnesol (7.5 μM −500- μM). Concentration response curve was generated using non-linear regression analysis using graph pad prism 9.0. The data represent SEM of at least three independent experiments performed in triplicate. Statistically significant values are shown with asterisk (*$p < 0.05$, **$p < 0.01$). G (iv). Effect of AIP-1 (50 μM) from *S. aureus* on calcium mobilization in BD, BCF HBEs. Intracellular calcium release in BD and BCF cells was measured following treatment with AIP-1 (50 μM). The data represents the SEM of at least three independent experiments performed in triplicate.

To evaluate if changes in AC activity could be linked to T2R14, we analyzed the direct interaction between T2R14 with Gαs and Gαi using a NanoBRET assay (See Figures S3B–S3D). Gαi had a specific and saturable association with T2R14 (Figure 2D). Gαs did not interact with T2R14 and gave results resembling the non-interacting negative control protein p53 (See Figure S3D). This finding indicates that enhanced T2R14 activation in CF may lead to greater inhibition of AC by Gαi and reduced cAMP production. To test if this cAMP response is T2R14-Gαi specific, BD and BCF cells were treated with the T2R14 specific agonist DPH at a range of concentrations in the presence or absence of TAT-GPR. TAT-GPR increased the DPH mediated cAMP response in BCF significantly, indicating that T2R14-Gαi signaling is enhanced in CF cells (Figure 2Ei-ii).

The effects of T2R14 agonists DPH, C12, AIP-1, tyrosol, and farnesol on cAMP responses revealed that these agonists attenuate forskolin-induced cAMP generation (Figures 2F and 2G) in non-CF HBE (BD) cells. By contrast, CF cells showed little

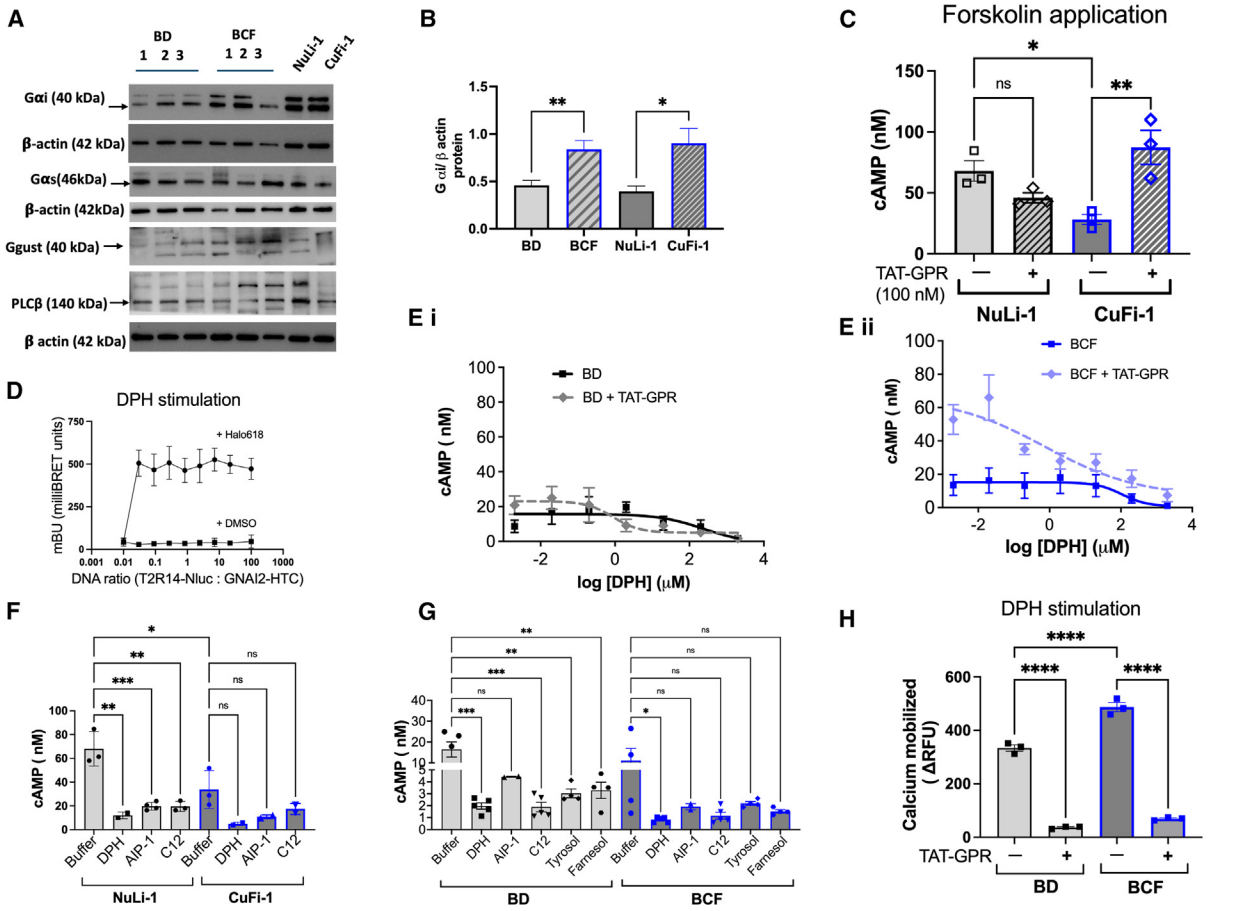

Figure 2. Gαi coupling to T2R14 enables downstream signaling responses to QSMs

(A) Western blot analysis of G-protein subunits. Expression of Gαi, Gαs and Ggust in CF (CuFi-1, BCF) and non-CF (NuLi-1, BD) cells. Image is representative of $n = 3$.

(B) Densitometric analysis showing Gαi expression in BD, BCF, NuLi-1 and CuFi-1 cells.

(C) Effect of Gαi inhibition on cAMP accumulation in non-CF (NuLi-1) and CF (CuFi-1) cells. Cells were stimulated with forskolin to stimulate cAMP production, in the absence or presence Gαi peptide blocker TAT-GPR (100 nM, 15 min) and cAMP levels assayed. Values are SEM from a minimum of $n = 3$ experiments.

(D) NanoBRET ratio was measured following DPH treatment (2mM, 5 min) of CHO-K1 cells that had been co-transfected with constant amount of plasmid encoding T2R14 with a C-terminal nanoluciferase tag (T2R14-sNLuc), combined with increasing amounts of plasmid encoding Gαi2 with C-terminal HaloTag (GNAI2-HTC). Cells were exposed to either Halo618 (black circles) or DMSO (black squares) and NanoBRET ratio measured. The T2R14-Gαi interaction reflects saturable binding. Data represent mean ± S.E.M from at least three replicates per experiment across three independent repeats.

(E) Dose-response curves for T2R14 specific agonist DPH showing cAMP levels in Forskolin-treated BD (i) and BCF (ii) HBE cells. Faint dotted lines represent cells treated with Gαi peptide blocker TAT-GPR and control is represented with dark solid lines.

(F) cAMP levels in HBE cell lines post T2R14 activation. cAMP was measured following stimulation with DPH, as well as QSMs AIP-1 and C12, and subsequently treated with Forskolin.

(G) cAMP levels in primary non-CF (BD) and CF (BCF) HBEs. Both BD and BCF cells were stimulated with DPH (500 μM), C12, AIP-1, farnesol or tyrosol following treatment with Forskolin.

(H) Calcium signaling in HBE cell lines upon pre-treatment with TAT-GPR peptide followed by DPH (500 μM) treatment. *$p < 0.05$, **$p < 0.01$, ***$p < 0.001$. Bar graph data are SEM from a minimum of $n = 3$ experiments.

cAMP accumulation following forskolin stimulation, congruent with the elevated Gαi in these cell types. These findings are consistent with the previous observation that T2R activation by *P. aeruginosa*-derived signals elevates intracellular calcium while reducing cAMP accumulation.[25] Signaling by the canonical T2Rs involves dissociation of Gα-gust from Gβγ-gust dimer to increase intracellular calcium via T2Rs-PLCβ2-IP_3-Ca^{2+} signaling. We assessed calcium mobilization in CF and non-CF cells and found that pre-treatment with TAT-GPR peptide blunted the calcium response to DPH in both CF and non-CF cells, indicating that Gαi may have a role in T2R14-mediated calcium signaling (Figure 2H).

T2R14 mediates innate immune responses in primary CF and non-CF HBEs

Nitric oxide (NO) levels are reduced in pwCF, and may reflect impaired production, increased metabolism, or a dysfunctional NO pathway that results from downregulation of NO synthase

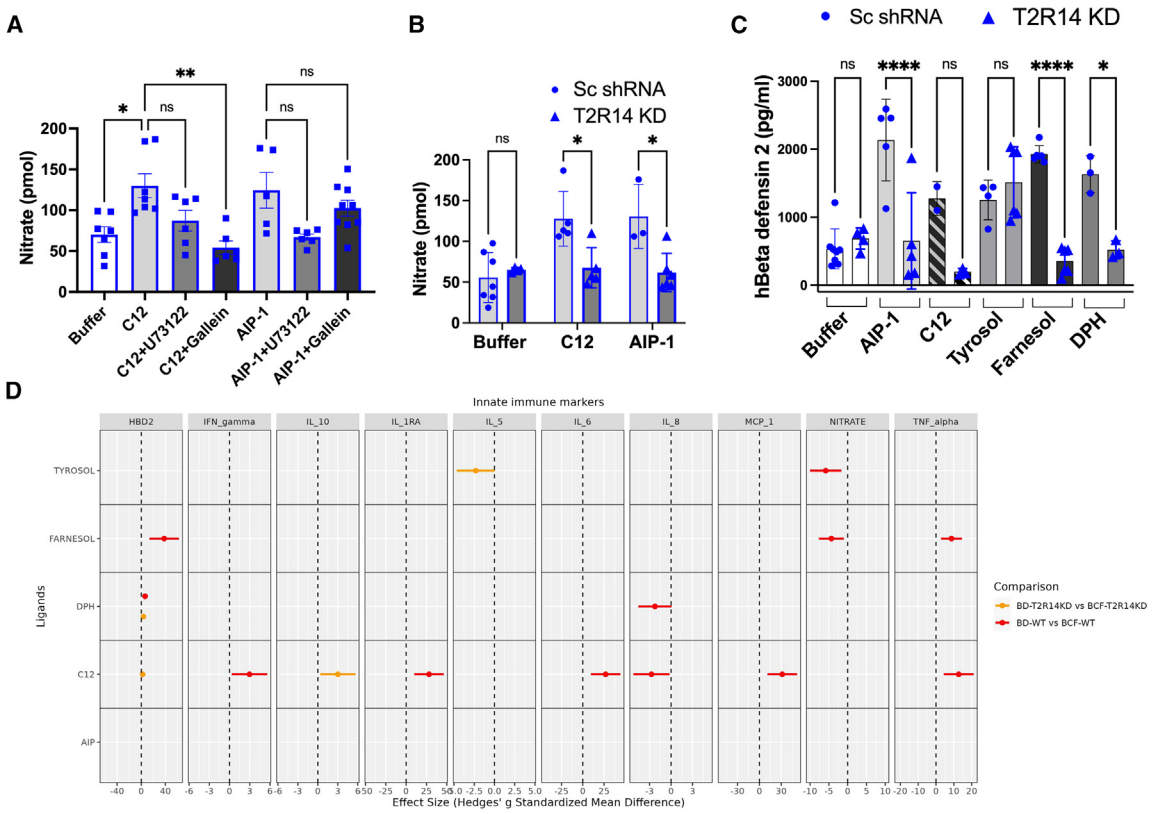

Figure 3. T2R14 mediated innate immune responses in primary CF and non-CF HBEs

(A and B) Nitrate release upon T2R14 stimulation. Total nitrate (NO_3^- + NO_2^-) release was assessed in ALI cultures of CF HBE cells transfected with either Sc shRNA or T2R14 KD cells. The apical surface was exposed to the T2R agonists C12 (100 μM), AIP-1 (50 μM) and the T2R downstream signaling inhibitors Gβγ (gallein, 10 μM) and PLCβ (U73122, 10 μM). (**$p < 0.01$, *$p < 0.05$ vs. buffer control; #$p < 0.05$ vs. treatment control without inhibitors). Data represents results from at least 3 independent experiments.

(C) Antimicrobial peptide (AMP) secretion upon T2R14 agonist stimulation. Human Beta defensin 2 (hBD2) secretion from BCF cells, transfected with Sc shRNA (blue circles) or T2R14 KD (blue triangles) and cultured at the ALI was assessed by ELISA, following stimulation of the cultures with bacterial or fungal QSMs as indicated.

(D) Forest plot of primary CF and non-CF HBEs comparing innate immune markers in control sc shRNA and T2R14KD groups. Fifteen cytokines were analyzed using the Eve Technologies 15-Plex discovery assay and eight cytokines were detected. These eight cytokines along with total nitrate and hDB2 from panels (A–C) were analyzed using Hedge's g standardized mean difference.

isozymes.[29] Moreover, previous studies have suggested that T2R38 induced NO production in airway epithelial cells is bactericidal against *P. aeruginosa*.[25] In the present work, we measured the nitrate/nitrite concentrations in supernatants from CF HBE cells cultured at ALI (Figure 3A). In these ALI cultures, the apical surface was exposed to different T2R agonists for 18 h. Subsequently, nitrate/nitrite levels were quantified in 40 μL samples of apical secretions using a fluorometric assay. A significant elevation of total nitrate release was detected in C12 treated CF ALI cultures compared to untreated controls (Figure 3A). AIP-1 treated cells exhibited a similar trend but did not reach statistical significance. To confirm the role of T2R14 signaling in antimicrobial responses, downstream inhibitors of different arms of the T2R14 signaling pathway were applied in combination with the bitter agonists. Gallein is an inhibitor that blocks the Gβγ subunit signaling of the phosphatidylinositol 3-kinase[30] and U73122 inhibits phospholipase C activity.[31] Both these inhibitors reduced the nitrate release evoked by C12, without altering the AIP-1 stimulated release significantly (Figure 3A). To further establish the role of T2R14 in these responses, we resorted to BCF cells in which T2R14 mRNA transcript levels were reduced using shRNA (validated earlier (Figures 1F and 1G)). T2R14 deficient CF cells displayed reduced total nitrate levels, highlighting the specific involvement of T2R14 (Figure 3B). Antimicrobial peptides (AMPs) such as human beta-defensin 2 (hBD-2) are cationic endogenous antibiotic proteins expressed by the airway mucosa and are important effectors of the innate immune system. Treating well-differentiated ALI cultures of BCF cells with QSMs enhanced the secretion of hBD-2 particularly in cells stimulated with AIP-1and farnesol. ALI cultures from T2R14 knockdown cells displayed a reduced hBD-2 response, providing further evidence for a specific role of T2R14 activity in the AMP secretion response to microbial QSMs (Figure 3C).

Innate immune responses to microbes include cytokine secretion along with NO and AMPs. To understand the role of CFTR and T2R14 (variables) in the innate immune response to

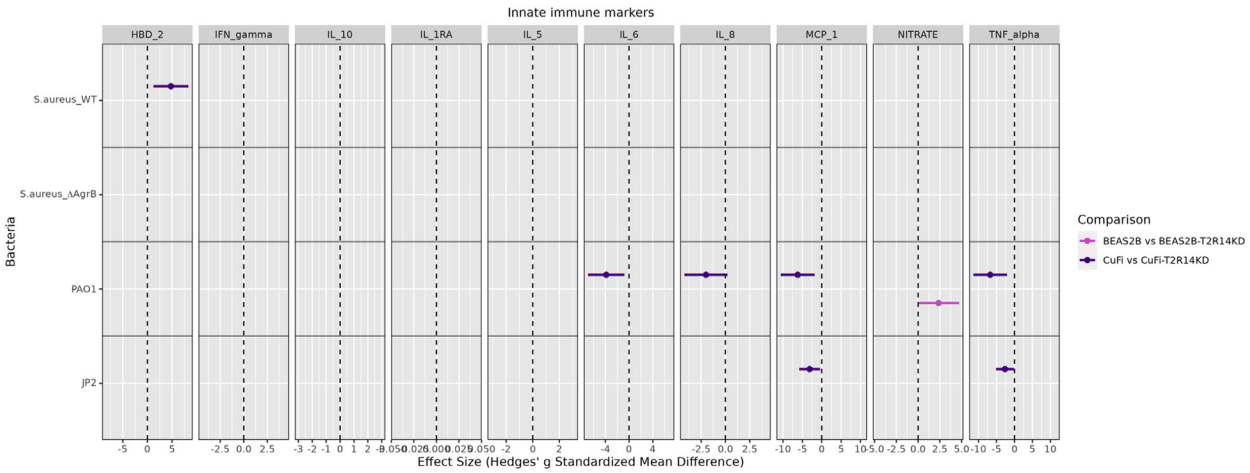

Figure 4. Innate immune responses to bacteria depend on T2R14 in CF epithelial cells

Forest plot comparing the effect of T2R14 KD in CF and non-CF cell lines on innate immune markers, upon challenge with live bacteria. Hedge's g standardized mean difference illustrates the effect of bacterial challenge (*P. aeruginosa* PAO1, *P. aeruginosa* JP2, *S. aureus* WT, *S. aureus* ΔagrB) on cytokine, hBD2, total nitrate and chemokine levels in WT and T2R14KD BEAS-2B and CuFi-1 cells.

CF-relevant QSMs (stimuli), we performed effect size measurement of individual innate immune markers and visualized these using forest plots (Figure 3D, and see STAR Methods). The effect size for innate immune responses, which included a panel of cytokines, AMP and total nitrate levels, was analyzed using Hedges' g standardized mean difference. Analysis of forest plots for innate immune markers in primary HBE cells of CF (BCF) and non-CF (BD) origin revealed a higher innate immune response to C12 in CF cells compared to wild type cells. However, IL-8 secretion was reduced in CF cells. Furthermore, IL-10 secretion was specifically upregulated in response to C12, in T2R14-deficient CF cells compared to T2R14-deficient non-CF cells. Farnesol and tyrosol stimulation elicited different innate immune responses in non-CF and CF cells, with intact T2R14; with CF condition being associated with increased TNF-α and hBD-2, and reduced total nitrate. The underlying changes in calcium and cAMP levels are visualized as forest plots (See Figure S4A). T2R14 deficient CF cells have a lower IL8 and IL10 response to AIP-1, as compared to T2R14 intact CF cells (See Figure S4B). Together these analyses indicate that distinct innate immune markers are upregulated in CF conditions in response to different QSMs, and the upregulation depends on T2R14.

Innate immune responses to bacterial challenge depend on T2R14 in CF HBE cell lines

We next examined the role of T2R signaling in modulating the innate immune system when faced with bacterial challenge. To test whether T2R14 plays an important in activation of innate immune responses to bacterial QSMs, we treated HBE cells with live, wild type *P. aeruginosa* and *S. aureus* and to QSM deficient control strains of both bacteria. The JP2 strain is a QS mutated form of *P. aeruginosa* (*ΔlasI*) which is unable to synthesize QSM C12. The QSM deficient strain of *S. aureus* (SAur*ΔAgrB*) was produced by deleting a segment of the *AgrB* gene using CRISPR, resulting in an inability to secrete AIP-1 (See Figure S5 and See STAR Methods Data S1 and Data S2). Consistent with preceding results, T2R14 deficient CuFi-1 cells exhibited a significant decrease in innate immune marker secretion compared to WT CuFi-1 cells (Figure 4, See Figure S4C). This effect was prevalent on treatment with wild type *P. aeruginosa*, and the effect was blunted in the QSM deficient strain (JP2) (See Figures S6A–S6E), indicating an important role for T2R14 in innate immune responses to *P. aeruginosa* in CF. Given that it is well established that VX-809 is able to at least partially rescue Cl-transport in pwCF who have ΔF508 CFTR mutation,[32] we tested whether the elevation in Gαi in ΔF508 CF cells, and the associated decreased levels of cAMP (Figure 2C), may be affected by VX-809 corrector therapy. Abbattiscianni et al.[33] have observed an increase in plasma membrane associated cAMP in CF HBEs treated with VX-809, however, we examined total cAMP. We have already shown that inhibition of Gαi with TAT-GPR leads to a rescue of cAMP levels (Figure 2C). Therefore, we sought to determine whether VX-809 corrector treatment is also associated with greater cAMP levels given an environment of higher Gαi. Our data show that CuFi-1 cells, treated with VX-809 for 24 h, showed a significant increase in cAMP levels in response to forskolin (See Figure S7). No significant change was detected in NuLi cells. Taken together, these data suggest a link between elevated Gαi and cAMP levels in pwCF that can be modified with corrector therapy.

DISCUSSION

Recent advances in the treatment of CF with CFTR modulators has dramatically improved health outcomes for pwCF. However, for people who cannot tolerate or do not respond to these treatments, there is an urgent need for novel therapeutics to alleviate the chronic lung infections that result from airway epithelial dysfunction and reduced mucociliary clearance. T2Rs have recently been identified as key players in the innate immune defense of the airways, with several early studies highlighting their potential as immune modulators against both Gram-positive and

Gram-negative pathogens.[11–13,25,34] Despite these initial findings, the specific role for T2Rs in CF remains unclear.

Our data identify T2R14 as an attractive target for innate immune-modulation in CF HBE cells. We find elevated transcription of TAS2R14 in CF compared to non-CF cells, which aligns with findings in other diseases such as asthma.[35,36] Higher T2R14 expression has also been reported in breast cancer[14,37] where it influences proliferation and migration of cancerous cells.[37] Previous studies have identified multiple T2Rs, including T2R4, T2R14, T2R16, and T2R38, in human airway epithelial cells, typically localized in ciliated bronchial epithelial cells; however, T2R14 seems to play a predominant role in host defense response under our conditions.

In the gustatory system, T2Rs are typically coupled with the G protein gustducin (Gαgust). A previous study showed that mice lacking Gαgust can still perceive bitter tastes, suggesting that T2Rs may signal through alternative Gα proteins beyond Gα gust.[38] Liggett et al., showed that Gαi is important for T2R-mediated signaling in airway smooth muscle cells where it causes intracellular calcium release that is crucial for bronchodilation and the relaxation—a process distinct from cAMP-mediated relaxation.[24] Consistent with those observations, we found using NanoBRET that T2R14 interacts specifically with Gαi, but not Gαs, when activated by the bitter agonist DPH. Further, treatment of CF cells with the Gαi blocker TAT-GPR peptide promoted cAMP accumulation and reduced calcium mobilization in response to DPH. Since TAT-GPR prevents the Gi trimer from associating with GPCRs, the Gαi subunit is not activated and consequently does not inhibit adenylyl cyclase. The reduction in calcium mobilization is probably due to the inability of the Gβγ dimer to dissociate from the Gi trimer, and therefore reduced activation of PLCβ.[39] In addition, a recent study using human embryonic kidney (HEK) cells reported T2R14-Gαi coupling and suggested that activation is mediated, in part, by Leucine^{201} [40] consistent with the observed role of Gαi downstream of T2R14.

To explore the role of T2R14 in CF, we interrogated molecules and pathways downstream of the receptor, and studied responses to QSMs from CF-related pathogens; in CF and non-CF cells. We detected elevated Gαi protein in CF cells, including the CuFi-1 cell line and BCF primary cells (Figure 2), while Gαs was unaffected. The elevated levels of Gαi protein would facilitate interactions with T2R14, amplifying the effects of agonists that stimulate Ca^{2+} signaling and inhibit the cAMP pathway. This notion is supported by the more pronounced reduction in calcium mobilization in DPH stimulated CF cells upon TAT-GPR treatment. The observation of elevated Gαi in primary samples and cell lines bearing the ΔF508 mutation in CFTR is consistent with independent observation using a CRISPR-approach in 16HBEo-cells, where engineering the ΔF508 mutation was correlated with an increase in the level of Gαi3 protein.[41] Transcriptional control of *GNAI* in CF-deficient cells is an interesting avenue for further exploration. A mechanism that might explain the increased Gαi expression in CF is the hypoxia that results from opportunistic infection by Gram-negative bacteria such as *P. aeruginosa*. This hypothesis is supported by studies like those from Kacimi et al., which observed an elevation of Gαi2 under chronic hypoxia in the right ventricle of rat hearts.[42] Alternatively, a pro-inflammatory state in CF characterized by lipid imbalance and increased IL-8 secretion, could be responsible for the elevated Gαi expression.[29,43,44] A third possibility is the regulation of NF-κB by CFTR. Already, in delF508 mouse intestinal epithelial cells, mutual interactions between CFTR, β-catenin and NF-κB have been detected[11–13,34,45] Mutation-specific effects on transcription of specific target genes (*GNAI* vs. *GNAS*) may provide new insights into *GNAI* overexpression in CF-mutant cells. Increased expression of *GNAI*, the gene that encodes Gαi could contribute to CF pathology through inhibition of adenylyl cyclases and generation of cAMP. In airway epithelia AC6 is a key isoform and has been identified as a regulator of mucociliary clearance.[46] Elevated expression of *GNAI* could suppress AC6 activity, thereby reducing mucociliary clearance. Approaches that specifically activate AC6 or prevent the interaction of AC6 with Gαi are therefore expected to help improve mucociliary clearance.

Host-pathogen interactions are complex and incompletely understood. Indeed, interkingdom signaling through QSMs may be of vital importance for the survival of host and/or bacteria/fungi. We selected QSMs from well-known CF airway pathogens (*P. aeruginosa, S. aureus and C. albicans*) to study innate immune activation through T2R14. Activation of T2R14 by Gram-negative bacterial QSMs and plant flavonoids has been implicated in the modulation of the innate immune response.[47] Using airway cells from chronic rhinosinusitis (CRS) patients, a previous study reported that T2R4 and T2R14 activation by *P. aeruginosa* quinolones, leads to reductions in basal cAMP levels and PKA activity.[25] Similarly, denatonium has been reported to decrease cAMP levels in response to forskolin in bronchial epithelial cells.[48] While these studies provided insights into T2Rs-mediated responses in CRS, they did not investigate altered responses of CF cells or the T2R14-specific agonist DPH.

A recent review on the cAMP and CFTR has highlighted the fact that pwCF exhibit varied responses to modulator therapy and that the possibility of modulating cAMP signaling complexes holds the potential to help pwCF who do not respond to modulator therapy. Modulation of cAMP could also serve to enhance the effects of current therapies.[49] We have shown that elevated Gαi in ΔF508 CF cells is associated with reduced cAMP and that VX-809 can lead to increases in cAMP in these cells.

Here, we have demonstrated that bacterial and fungal QSMs signal through T2R14 in airway epithelium (Figure 1G(i-iii) and impact several immune markers. Total nitrate production (as proxy of NO) was regulated in part by T2R14 bound to C12 and AIP-1 in CF HBEs, however no difference was found between CF and non-CF groups. This finding is buttressed by other research[50] indicating that T2R agonists do not modify nitrate levels in epithelial cells, where the immune response is cAMP-dependent. Interestingly, CF HBEs exhibited reduced nitrate secretion in response to fungal QSMs, farnesol and tyrosol (Figure 3D). This reduction in antimicrobial response in CF cells may help to explain why some fungi persist in the airway as the complex microbial microenvironment may modify host response to enable survival. The precise details that contribute to differences in response to distinct QSMs, and between CF- and non-CF cells, remain to be elucidated. This may be related to difference in the spatial distribution such that most of CFTR in found in

ionocytes.[51] Even among ciliated cells that may co-express CFTR and T2R14, T2R14 is localized in the cilia, while recent work suggests that CFTR is unlikely to be present in the same vicinity.[52] The interactions linking T2R14 and CFTR remain to be identified and characterized.

Challenge with live bacteria revealed a distinct reduction of T2R14 dependent innate immune responses in CF cell lines treated with wild-type *P. aeruginosa*, which were minimized or eliminated in a QS deficient strain of *P. aeruginosa* (Figure 4). These reductions were not evident on treatment with C12 QSMs (Figure S4B) suggesting that additional T2R14 responsive elements may be secreted by *P. aeruginosa*.

In conclusion, through this comprehensive study, we have established the pivotal role of T2R14 in modulating the innate immune defense of CF airway epithelial cells. The research has revealed the elevated expression of Gαi in CF cells and consequential decrease in cAMP levels. Downstream effects of this T2R14 signaling cascade would likely include increases in calcium mobilization, NO production, IL-8 secretion, and hBD-2 production. Lastly, the results suggest a complex network in which T2R14 may impact key immune processes and responses, through its influence on Gαi-mediated signaling, highlighting the potential of interactions between T2R14, Gαi and AC6 as novel therapeutic targets for respiratory diseases.

Limitations of the study

The study analyzed a small sample of CF and non-CF. No knockdown fungal strains were used. The knockdown of T2R14 was not 100% in CF and non-CF cells. The study did not analyze T2R signaling under hypoxia which might be physiologically relevant in CF. It is possible that in addition to T2R14 there might be other G protein-coupled receptors that signal through Gαi, and whether they cause similar effects as T2R14 needs to be analyzed. Further mechanistic studies are needed to reveal how VX-809 increases cAMP and the potential of Gαi modulation to improve CFTR function. As this paper is directed at innate immunity defects in pwCF and the possible link between T2R14 and Gαi signaling, as opposed to direct CFTR channel functional consequences, our data are limited to cAMP as an indicator of the potential effects on CFTR channel activity. Future studies will need to address this limitation by examining CFTR function directly through membrane potential or patch clamp assays.

RESOURCE AVAILABILITY

Lead contact

Further information should be directed to Dr. Prashen Chelikani (Prashen.Chelikani@umanitoba.ca).

Materials availability

This study did not generate new unique reagents. Further information and requests for resources and reagents should be directed to Dr. Prashen Chelikani (Prashen.Chelikani@umanitoba.ca).

Data and code availability

- This study does not report original code.
- Any additional information required to reanalyze the data in this paper is available from the lead contact upon request.
- This study does not report any accession codes. Other data related to the current study is available from the lead contact upon request.

ACKNOWLEDGMENTS

This work was supported financially by a research grant from the Cystic Fibrosis Foundation (003100G221-Chelikani).

AUTHOR CONTRIBUTIONS

Conceptualization, N.S., and P.C.; Methodology and Formal analysis, N.S., R.H.C., A.Y.C., A.V., T.G., and P.C.; Investigation, N.S., R.H.C., A.Y.C., A.V., W.M.K., and T.G.; Resources, W.M.K., K.D., and J.W.H.; Data curation, N.S., R.H.C., A.V., and T.G.; Writing – Original Draft, N.S., R.H.C., A.Y.C., A.V., T.G., and P.C.; Writing – Review and Editing, N.S., R.H.C., A.Y.C., A.V., W.M.K., T.G., K.D., A.S.G., S.D., J.W.H., and P.C.; Visualization, A.Y.C. and A.V.; Supervision, S.D., and P.C.; Project Administration, P.C.; Funding Acquisition, K.D., A.S.G., and P.C.

DECLARATION OF INTERESTS

The authors declare no competing interests.

STAR★METHODS

Detailed methods are provided in the online version of this paper and include the following:

- KEY RESOURCES TABLE
- EXPERIMENTAL MODEL AND STUDY PARTICIPANT DETAILS
  - Cell lines and primary cells used in the study
  - Bacterial strains used in the study
- METHOD DETAILS
  - Co-culture assay on CF and non-CF HBE monolayer cells
  - Generation of primary human airway epithelial airway-liquid interface (ALI) cultures
  - Knockdown of T2R14 in CuFi-1, BEAS-2B and primary airway bronchial epithelial BD (non-CF) and BCF (CF) cells using shRNA lentiviral system
  - Immunoblot analysis
  - NanoBRET
  - Intracellular calcium mobilization assay
  - Determination of intracellular cAMP
  - Measurement of nitrate/nitrite secretion
  - Human β-Defensin 2 (hBD-2) ELISA
  - Measurement of secreted cytokines (multiplexing) by eve technologies
  - Real time quantitative PCR (qPCR) method
  - CRISPR protocol for the construction of the *agrBD* mutant of *S. aureus*, related to Figure S5
- QUANTIFICATION AND STATISTICAL ANALYSIS

SUPPLEMENTAL INFORMATION

Supplemental information can be found online at https://doi.org/10.1016/j.isci.2024.111286.

Received: December 12, 2023
Revised: April 30, 2024
Accepted: October 28, 2024
Published: October 30, 2024

REFERENCES

1. Cutting, G.R. (2015). Cystic fibrosis genetics: from molecular understanding to clinical application. Nat. Rev. Genet. *16*, 45–56. https://doi.org/10.1038/nrg3849.
2. Bhagirath, A.Y., Li, Y., Somayajula, D., Dadashi, M., Badr, S., and Duan, K. (2016). Cystic fibrosis lung environment and Pseudomonas aeruginosa

infection. BMC Pulm. Med. *16*, 174. https://doi.org/10.1186/s12890-016-0339-5.

3. Schwarz, C., Eschenhagen, P., and Bouchara, J.P. (2021). Emerging Fungal Threats in Cystic Fibrosis. Mycopathologia *186*, 639–653. https://doi.org/10.1007/s11046-021-00574-w.
4. Wang, Y., Bian, Z., and Wang, Y. (2022). Biofilm formation and inhibition mediated by bacterial quorum sensing. Appl. Microbiol. Biotechnol. *106*, 6365–6381. https://doi.org/10.1007/s00253-022-12150-3.
5. Mehmood, A., Liu, G., Wang, X., Meng, G., Wang, C., and Liu, Y. (2019). Fungal Quorum-Sensing Molecules and Inhibitors with Potential Antifungal Activity: A Review. Molecules *24*, 1950. https://doi.org/10.3390/molecules24101950.
6. Wang, X., Zhang, Z., Louboutin, J.P., Moser, C., Weiner, D.J., and Wilson, J.M. (2003). Airway epithelia regulate expression of human beta-defensin 2 through Toll-like receptor 2. Faseb. J. *17*, 1727–1729. https://doi.org/10.1096/fj.02-0616fje.
7. Shaykhiev, R., Behr, J., and Bals, R. (2008). Microbial patterns signaling via Toll-like receptors 2 and 5 contribute to epithelial repair, growth and survival. PLoS One *3*, e1393. https://doi.org/10.1371/journal.pone.0001393.
8. Szul, T., Bratcher, P.E., Fraser, K.B., Kong, M., Tirouvanziam, R., Ingersoll, S., Sztul, E., Rangarajan, S., Blalock, J.E., Xu, X., and Gaggar, A. (2016). Toll-Like Receptor 4 Engagement Mediates Prolyl Endopeptidase Release from Airway Epithelia via Exosomes. Am. J. Respir. Cell Mol. Biol. *54*, 359–369. https://doi.org/10.1165/rcmb.2015-0108OC.
9. Losol, P., Ji, M.H., Kim, J.H., Choi, J.P., Yun, J.E., Seo, J.H., Kim, B.K., Chang, Y.S., and Kim, S.H. (2023). Bronchial epithelial cells release inflammatory markers linked to airway inflammation and remodeling in response to TLR5 ligand flagellin. World Allergy Organ. J. *16*, 100786. https://doi.org/10.1016/j.waojou.2023.100786.
10. Crossen, A.J., Ward, R.A., Reedy, J.L., Surve, M.V., Klein, B.S., Rajagopal, J., and Vyas, J.M. (2022). Human Airway Epithelium Responses to Invasive Fungal Infections: A Critical Partner in Innate Immunity. J. Fungi *9*, 40. https://doi.org/10.3390/jof9010040.
11. Medapati, M.R., Singh, N., Bhagirath, A.Y., Duan, K., Triggs-Raine, B., Batista, E.L., Jr., and Chelikani, P. (2021). Bitter taste receptor T2R14 detects quorum sensing molecules from cariogenic Streptococcus mutans and mediates innate immune responses in gingival epithelial cells. Faseb. J. *35*, e21375. https://doi.org/10.1096/fj.202000208R.
12. Carey, R.M., Palmer, J.N., Adappa, N.D., and Lee, R.J. (2023). Loss of CFTR function is associated with reduced bitter taste receptor-stimulated nitric oxide innate immune responses in nasal epithelial cells and macrophages. Front. Immunol. *14*, 1096242. https://doi.org/10.3389/fimmu.2023.1096242.
13. Lee, R.J., and Cohen, N.A. (2015). Taste receptors in innate immunity. Cell. Mol. Life Sci. *72*, 217–236. https://doi.org/10.1007/s00018-014-1736-7.
14. Jaggupilli, A., Singh, N., Upadhyaya, J., Sikarwar, A.S., Arakawa, M., Dakshinamurti, S., Bhullar, R.P., Duan, K., and Chelikani, P. (2017). Analysis of the expression of human bitter taste receptors in extraoral tissues. Mol. Cell. Biochem. *426*, 137–147. https://doi.org/10.1007/s11010-016-2902-z.
15. Medapati, M.R., Bhagirath, A.Y., Singh, N., and Chelikani, P. (2022). Pharmacology of T2R Mediated Host-Microbe Interactions. Handb. Exp. Pharmacol. *275*, 177–202. https://doi.org/10.1007/164_2021_435.
16. Ramage, G., Saville, S.P., Wickes, B.L., and López-Ribot, J.L. (2002). Inhibition of Candida albicans biofilm formation by farnesol, a quorum-sensing molecule. Appl. Environ. Microbiol. *68*, 5459–5463. https://doi.org/10.1128/AEM.68.11.5459-5463.2002.
17. Alem, M.A.S., Oteef, M.D.Y., Flowers, T.H., and Douglas, L.J. (2006). Production of tyrosol by Candida albicans biofilms and its role in quorum sensing and biofilm development. Eukaryot. Cell *5*, 1770–1779. https://doi.org/10.1128/EC.00219-06.
18. Fang, Y., Wu, C., Wang, Q., and Tang, J. (2019). Farnesol contributes to intestinal epithelial barrier function by enhancing tight junctions via the JAK/STAT3 signaling pathway in differentiated Caco-2 cells. J. Bioenerg. Biomembr. *51*, 403–412. https://doi.org/10.1007/s10863-019-09817-4.
19. Arias, L.S., Delbem, A.C.B., Fernandes, R.A., Barbosa, D.B., and Monteiro, D.R. (2016). Activity of tyrosol against single and mixed-species oral biofilms. J. Appl. Microbiol. *120*, 1240–1249. https://doi.org/10.1111/jam.13070.
20. Leonhardt, I., Spielberg, S., Weber, M., Albrecht-Eckardt, D., Bläss, M., Claus, R., Barz, D., Scherlach, K., Hertweck, C., Löffler, J., et al. (2015). The fungal quorum-sensing molecule farnesol activates innate immune cells but suppresses cellular adaptive immunity. mBio *6*, e00143. https://doi.org/10.1128/mBio.00143-15.
21. Chandrashekar, J., Mueller, K.L., Hoon, M.A., Adler, E., Feng, L., Guo, W., Zuker, C.S., and Ryba, N.J. (2000). T2Rs function as bitter taste receptors. Cell *100*, 703–711.
22. Ruiz-Avila, L., McLaughlin, S.K., Wildman, D., McKinnon, P.J., Robichon, A., Spickofsky, N., and Margolskee, R.F. (1995). Coupling of bitter receptor to phosphodiesterase through transducin in taste receptor cells. Nature *376*, 80–85. https://doi.org/10.1038/376080a0.
23. Sainz, E., Cavenagh, M.M., Gutierrez, J., Battey, J.F., Northup, J.K., and Sullivan, S.L. (2007). Functional characterization of human bitter taste receptors. Biochem. J. *403*, 537–543.
24. Kim, D., Woo, J.A., Geffken, E., An, S.S., and Liggett, S.B. (2017). Coupling of Airway Smooth Muscle Bitter Taste Receptors to Intracellular Signaling and Relaxation Is via G(alphai1,2,3). Am. J. Respir. Cell Mol. Biol. *56*, 762–771. https://doi.org/10.1165/rcmb.2016-0373OC.
25. Freund, J.R., Mansfield, C.J., Doghramji, L.J., Adappa, N.D., Palmer, J.N., Kennedy, D.W., Reed, D.R., Jiang, P., and Lee, R.J. (2018). Activation of airway epithelial bitter taste receptors by Pseudomonas aeruginosa quinolones modulates calcium, cyclic-AMP, and nitric oxide signaling. J. Biol. Chem. *293*, 9824–9840. https://doi.org/10.1074/jbc.RA117.001005.
26. Shah, A.S., Ben-Shahar, Y., Moninger, T.O., Kline, J.N., and Welsh, M.J. (2009). Motile cilia of human airway epithelia are chemosensory. Science *325*, 1131–1134. https://doi.org/10.1126/science.1173869.
27. Sharma, P., Conaway, S., Jr., and Deshpande, D. (2022). Bitter Taste Receptors in the Airway Cells Functions. Handb. Exp. Pharmacol. *275*, 203–227. https://doi.org/10.1007/164_2021_436.
28. Appleton, K.M., Bigham, K.J., Lindsey, C.C., Hazard, S., Lirjoni, J., Parnham, S., Hennig, M., and Peterson, Y.K. (2014). Development of inhibitors of heterotrimeric Galphai subunits. Bioorg. Med. Chem. *22*, 3423–3434. https://doi.org/10.1016/j.bmc.2014.04.035.
29. Andersson, C., Al-Turkmani, M.R., Savaille, J.E., Alturkmani, R., Katrangi, W., Cluette-Brown, J.E., Zaman, M.M., Laposata, M., and Freedman, S.D. (2008). Cell culture models demonstrate that CFTR dysfunction leads to defective fatty acid composition and metabolism. J. Lipid Res. *49*, 1692–1700. https://doi.org/10.1194/jlr.M700388-JLR200.
30. Lehmann, D.M., Seneviratne, A.M.P.B., and Smrcka, A.V. (2008). Small molecule disruption of G protein beta gamma subunit signaling inhibits neutrophil chemotaxis and inflammation. Mol. Pharmacol. *73*, 410–418. https://doi.org/10.1124/mol.107.041780.
31. Bleasdale, J.E., Bundy, G.L., Bunting, S., Fitzpatrick, F.A., Huff, R.M., Sun, F.F., and Pike, J.E. (1989). Inhibition of phospholipase C dependent processes by U-73, 122. Adv. Prostaglandin Thromboxane Leukot. Res. *19*, 590–593.
32. Ren, H.Y., Grove, D.E., De La Rosa, O., Houck, S.A., Sopha, P., Van Goor, F., Hoffman, B.J., and Cyr, D.M. (2013). VX-809 corrects folding defects in cystic fibrosis transmembrane conductance regulator protein through action on membrane-spanning domain 1. Mol. Biol. Cell *24*, 3016–3024. https://doi.org/10.1091/mbc.E13-05-0240.
33. Abbattiscianni, A.C., Favia, M., Mancini, M.T., Cardone, R.A., Guerra, L., Monterisi, S., Castellani, S., Laselva, O., Di Sole, F., Conese, M., et al.

(2016). Correctors of mutant CFTR enhance subcortical cAMP-PKA signaling through modulating ezrin phosphorylation and cytoskeleton organization. J. Cell Sci. *129*, 1128–1140. https://doi.org/10.1242/jcs.177907.

34. Lee, R.J., Kofonow, J.M., Rosen, P.L., Siebert, A.P., Chen, B., Doghramji, L., Xiong, G., Adappa, N.D., Palmer, J.N., Kennedy, D.W., et al. (2014). Bitter and sweet taste receptors regulate human upper respiratory innate immunity. J. Clin. Invest. *124*, 1393–1405. https://doi.org/10.1172/JCI72094.
35. Orsmark-Pietras, C., James, A., Konradsen, J.R., Nordlund, B., Söderhäll, C., Pulkkinen, V., Pedroletti, C., Daham, K., Kupczyk, M., Dahlén, B., et al. (2013). Transcriptome analysis reveals upregulation of bitter taste receptors in severe asthmatics. Eur. Respir. J. *42*, 65–78. https://doi.org/10.1183/09031936.00077712.
36. Yoon, S.Y., Shin, E.S., Park, S.Y., Kim, S., Kwon, H.S., Cho, Y.S., Moon, H.B., and Kim, T.B. (2016). Association between Polymorphisms in Bitter Taste Receptor Genes and Clinical Features in Korean Asthmatics. Respiration *91*, 141–150. https://doi.org/10.1159/000443796.
37. Singh, N., Shaik, F.A., Myal, Y., and Chelikani, P. (2020). Chemosensory bitter taste receptors T2R4 and T2R14 activation attenuates proliferation and migration of breast cancer cells. Mol. Cell. Biochem. *465*, 199–214. https://doi.org/10.1007/s11010-019-03679-5.
38. Caicedo, A., Pereira, E., Margolskee, R.F., and Roper, S.D. (2003). Role of the G-protein subunit alpha-gustducin in taste cell responses to bitter stimuli. J. Neurosci. *23*, 9947–9952.
39. Ferry, X., Eichwald, V., Daeffler, L., and Landry, Y. (2001). Activation of betagamma subunits of G(i2) and G(i3) proteins by basic secretagogues induces exocytosis through phospholipase Cbeta and arachidonate release through phospholipase Cgamma in mast cells. J. Immunol. *167*, 4805–4813. https://doi.org/10.4049/jimmunol.167.9.4805.
40. Bloxham, C.J., Hulme, K.D., Fierro, F., Fercher, C., Pegg, C.L., O'Brien, S.L., Foster, S.R., Short, K.R., Furness, S.G.B., Reichelt, M.E., et al. (2024). Cardiac human bitter taste receptors contain naturally occurring variants that alter function. Biochem. Pharmacol. *219*, 115932. https://doi.org/10.1016/j.bcp.2023.115932.
41. Santos, L., Nascimento, R., Duarte, A., Railean, V., Amaral, M.D., Harrison, P.T., Gama-Carvalho, M., and Farinha, C.M. (2023). Mutation-class dependent signatures outweigh disease-associated processes in cystic fibrosis cells. Cell Biosci. *13*, 26. https://doi.org/10.1186/s13578-023-00975-y.
42. Kacimi, R., Moalic, J.M., Aldashev, A., Vatner, D.E., Richalet, J.P., and Crozatier, B. (1995). Differential regulation of G protein expression in rat hearts exposed to chronic hypoxia. Am. J. Physiol. *269*, H1865–H1873. https://doi.org/10.1152/ajpheart.1995.269.6.H1865.
43. Garić, D., De Sanctis, J.B., Dumut, D.C., Shah, J., Pena, M.J., Youssef, M., Petrof, B.J., Kopriva, F., Hanrahan, J.W., Hajduch, M., and Radzioch, D. (2020). Fenretinide favorably affects mucins (MUC5AC/MUC5B) and fatty acid imbalance in a manner mimicking CFTR-induced correction. Biochim. Biophys. Acta Mol. Cell Biol. Lipids *1865*, 158538. https://doi.org/10.1016/j.bbalip.2019.158538.
44. Dean, T.P., Dai, Y., Shute, J.K., Church, M.K., and Warner, J.O. (1993). Interleukin-8 concentrations are elevated in bronchoalveolar lavage, sputum, and sera of children with cystic fibrosis. Pediatr. Res. *34*, 159–161. https://doi.org/10.1203/00006450-199308000-00010.
45. Liu, K., Zhang, X., Zhang, J.T., Tsang, L.L., Jiang, X., and Chan, H.C. (2016). Defective CFTR- beta-catenin interaction promotes NF-kappaB nuclear translocation and intestinal inflammation in cystic fibrosis. Oncotarget *7*, 64030–64042. https://doi.org/10.18632/oncotarget.11747.
46. Arora, K., Lund, J.R., Naren, N.A., Zingarelli, B., and Naren, A.P. (2020). AC6 regulates the microtubule-depolymerizing kinesin KIF19A to control ciliary length in mammals. J. Biol. Chem. *295*, 14250–14259. https://doi.org/10.1074/jbc.RA120.013703.
47. Hariri, B.M., McMahon, D.B., Chen, B., Freund, J.R., Mansfield, C.J., Doghramji, L.J., Adappa, N.D., Palmer, J.N., Kennedy, D.W., Reed, D.R., et al. (2017). Flavones modulate respiratory epithelial innate immunity: Anti-inflammatory effects and activation of the T2R14 receptor. J. Biol. Chem. *292*, 8484–8497. https://doi.org/10.1074/jbc.M116.771949.
48. Hollenhorst, M.I., Kumar, P., Zimmer, M., Salah, A., Maxeiner, S., Elhawy, M.I., Evers, S.B., Flockerzi, V., Gudermann, T., Chubanov, V., et al. (2022). Taste Receptor Activation in Tracheal Brush Cells by Denatonium Modulates ENaC Channels via Ca(2+). Cells *11*, 2411. https://doi.org/10.3390/cells11152411.
49. Murabito, A., Bhatt, J., and Ghigo, A. (2023). It Takes Two to Tango! Protein-Protein Interactions behind cAMP-Mediated CFTR Regulation. Int. J. Mol. Sci. *24*, 10538. https://doi.org/10.3390/ijms241310538.
50. Medapati, M.R., Bhagirath, A.Y., Singh, N., Schroth, R.J., Bhullar, R.P., Duan, K., and Chelikani, P. (2021). Bitter Taste Receptor T2R14 Modulates Gram-Positive Bacterial Internalization and Survival in Gingival Epithelial Cells. Int. J. Mol. Sci. *22*, 9920. https://doi.org/10.3390/ijms22189920.
51. Shah, V.S., Chivukula, R.R., Lin, B., Waghray, A., and Rajagopal, J. (2022). Cystic Fibrosis and the Cells of the Airway Epithelium: What Are Ionocytes and What Do They Do? Annu. Rev. Pathol. *17*, 23–46. https://doi.org/10.1146/annurev-pathol-042420-094031.
52. Sato, Y., Mustafina, K.R., Luo, Y., Martini, C., Thomas, D.Y., Wiseman, P.W., and Hanrahan, J.W. (2021). Nonspecific binding of common anti-CFTR antibodies in ciliated cells of human airway epithelium. Sci. Rep. *11*, 23256. https://doi.org/10.1038/s41598-021-02420-x.
53. Klabunde, B., Wesener, A., Bertrams, W., Ringshandl, S., Halder, L.D., Vollmeister, E., Schmeck, B., and Benedikter, B.J. (2023). Streptococcus pneumoniae disrupts the structure of the golgi apparatus and subsequent epithelial cytokine response in an H(2)O(2)-dependent manner. Cell Commun. Signal. *21*, 208. https://doi.org/10.1186/s12964-023-01233-x.
54. Jaggupilli, A., Singh, N., Jesus, V.C.D., Duan, K., and Chelikani, P. (2018). Characterization of the Binding Sites for Bacterial Acyl Homoserine Lactones (AHLs) on Human Bitter Taste Receptors (T2Rs). ACS Infect. Dis. *4*, 1146–1156. https://doi.org/10.1021/acsinfecdis.8b00094.
55. Higgins, G., Fustero Torre, C., Tyrrell, J., McNally, P., Harvey, B.J., and Urbach, V. (2016). Lipoxin A4 prevents tight junction disruption and delays the colonization of cystic fibrosis bronchial epithelial cells by Pseudomonas aeruginosa. Am. J. Physiol. Lung Cell Mol. Physiol. *310*, L1053–L1061. https://doi.org/10.1152/ajplung.00368.2015.
56. Lee, M.K., Yoo, J.W., Lin, H., Kim, Y.S., Kim, D.D., Choi, Y.M., Park, S.K., Lee, C.H., and Roh, H.J. (2005). Air-liquid interface culture of serially passaged human nasal epithelial cell monolayer for *in vitro* drug transport studies. Drug Deliv. *12*, 305–311. https://doi.org/10.1080/10717540500177009.
57. Waller, T.C., Berg, J.A., Lex, A., Chapman, B.E., and Rutter, J. (2020). Compartment and hub definitions tune metabolic networks for metabolomic interpretations. GigaScience *9*, giz137. https://doi.org/10.1093/gigascience/giz137.
58. Zuris, J.A., Thompson, D.B., Shu, Y., Guilinger, J.P., Bessen, J.L., Hu, J.H., Maeder, M.L., Joung, J.K., Chen, Z.Y., and Liu, D.R. (2015). Cationic lipid-mediated delivery of proteins enables efficient protein-based genome editing *in vitro* and *in vivo*. Nat. Biotechnol. *33*, 73–80. https://doi.org/10.1038/nbt.3081.
59. Rapiteanu, R., Karagyozova, T., Zimmermann, N., Singh, K., Wayne, G., Martufi, M., Belyaev, N.N., Hessel, E.M., Michalovich, D., Macarron, R., et al. (2020). Highly efficient genome editing in primary human bronchial epithelial cells differentiated at air-liquid interface. Eur. Respir. J. *55*, 1900950. https://doi.org/10.1183/13993003.00950-2019.
60. Pydi, S.P., Sobotkiewicz, T., Billakanti, R., Bhullar, R.P., Loewen, M.C., and Chelikani, P. (2014). Amino acid derivatives as bitter taste receptor (T2R) blockers. J. Biol. Chem. *289*, 25054–25066. https://doi.org/10.1074/jbc.M114.576975.

61. Nørskov-Lauritsen, L., Thomsen, A.R.B., and Bräuner-Osborne, H. (2014). G Protein-Coupled Receptor Signaling Analysis Using Homogenous Time-Resolved Förster Resonance Energy Transfer (HTRF®) Technology. Int. J. Mol. Sci. *15*, 2554–2572.

62. Foster, S.R., Hauser, A.S., Vedel, L., Strachan, R.T., Huang, X.P., Gavin, A.C., Shah, S.D., Nayak, A.P., Haugaard-Kedström, L.M., Penn, R.B., et al. (2019). Discovery of Human Signaling Systems: Pairing Peptides to G Protein-Coupled Receptors. Cell *179*, 895–908.e21. https://doi.org/10.1016/j.cell.2019.10.010.

63. Kimple, R.J., Kimple, M.E., Betts, L., Sondek, J., and Siderovski, D.P. (2002). Structural determinants for GoLoco-induced inhibition of nucleotide release by Galpha subunits. Nature *416*, 878–881. https://doi.org/10.1038/416878a.

64. Peterson, Y.K., Bernard, M.L., Ma, H., Hazard, S., 3rd, Graber, S.G., and Lanier, S.M. (2000). Stabilization of the GDP-bound conformation of Gialpha by a peptide derived from the G-protein regulatory motif of AGS3. J. Biol. Chem. *275*, 33193–33196. https://doi.org/10.1074/jbc.C000509200.

65. Chen, W., Zhang, Y., Yeo, W.S., Bae, T., and Ji, Q. (2017). Rapid and Efficient Genome Editing in Staphylococcus aureus by Using an Engineered CRISPR/Cas9 System. J. Am. Chem. Soc. *139*, 3790–3795. https://doi.org/10.1021/jacs.6b13317.

STAR★METHODS

KEY RESOURCES TABLE

REAGENT or RESOURCE	SOURCE	IDENTIFIER
Antibodies		
GNAT3	Novus Biologicals	Cat# NBP3-05122; RRID: AB_3533283
PLCβ2	Novus Biologicals	Cat# NBP2-93815; RRID: AB_3463750
G alpha i	Santa Cruz	Cat # SC-7276; RRID: AB_2111472
G alpha s	ProteinTech	Cat # 66253; RRID: AB_2935048
T2R14	Life Technologies	Cat # OSR00161W; RRID: AB_2201085
Beta 2 Adrenergic receptor	Bio Rad	Cat # MCA2784; RRID: AB_10848357
Beta actin	Sigma Aldrich	Cat # A5441; RRID: AB_10848357
Bacterial and virus strains		
S. aureus	*ATCC*	*6538*
P. aeruginosa PAO1	Dr. Kangmin Duan	N/A
S. aureus ΔAGR B	This study	N/A
P. aeruginosa JP2	Dr. Kangmin Duan	N/A
Chemicals, peptides, and recombinant proteins		
TAT-GPR	Kerafast	ESC101
C12	Sigma	09139-10MG
AIP-1	Bachem	4059504
Tyrosol	Sigma	188255-5G
Farnesol	Sigma	F203-25G
Forskolin	Sigma	F3917-10MG
IBMX	Thermo Scientific	J64598.MC
Diphenhydramine	Sigma	D3630-50G
Collagen Type I (Rat tail)	Corning	354236
Collagen Type IV	Sigma	C7521
PneumaCult Ex Plus	Stem Cell Tech	05041
PneumaCult ALI	Stem Cell Tech	05002
BEBM	Lonza	CC-3171
Opti-MEM	Gibco	51985-034
Lipofectamine 2000	Invitrogen	1668.019
BioRad DC kit	BioRad	5000113-5000115
ECL clarity	BioRad	170-5060
DMSO	Sigma	D2650-100ml
XhoI	NEB	R0146S
XbaI	NEB	R0145S
BsaI-HFv2	NEB	R3733S
rCutsmart 10X	NEB	B6004S
Kanamycin	Sigma	K1377
NEBuilder HiFi DNA Assembly Master Mix	NEB	E2621S
Luria-Bertani broth	Fisher Scientific	BP9723-500
Luria-Bertani agar	Fisher scientific	BP1425500
Gene Pulser Cuvette mini pack	Bio Rad	1652082
Tryptic soy broth	Fisher Scientific	B11768
Tryptic soy agar	Fisher Scientific	BP1423-500
DNeasy PowerSoil Pro Kit (250)	Qiagen	47016

(*Continued on next page*)

Continued

REAGENT or RESOURCE	SOURCE	IDENTIFIER
Chloramphenicol	Sigma	C0378-25G
Critical commercial assays		
Human β-defensin 2 (hBD-2) ELISA kit	PeproTech	900-K172
Nitrate/nitrite fluorometric assay kit	Cayman Chemical Company	780051
Gαi based cAMP homogeneous time-resolved fluorescence (HTRF) kit	Cisbio international	62AM9PEB
Fluo -4 NW kit	Life Technologies	F36206
Experimental models: Cell lines		
CHOK1 cells	ATCC	CCL-61
NuLi-1	ATCC	CRL-4011
CuFi-1	ATCC	CRL-4013
HEK 293 T cells	ATCC	University of Manitoba
BD (non-CF) and BCF (CF)	CFTRC, McGill	McGill University
Oligonucleotides		
Primer: T2R14 F - AAATATCCGGAGACGCCAGC R - CCTCCAACCTTTCAGAGGTCC	Life Technologies	Customized
GAPDH- F - CAATGACCCCTTCATTGACC R - ACCCAGAAGACTGTGGATGG	Life Technologies	Customized
T2R14 shRNA	Santa Cruz	sc-95889-V
Control shRNA	Santa Cruz	sc-108080
Primer: Beta 2 AR F- CTGCAGACGTCACCAACTA R- CCAGAAGTTGCCAAAAGTCC	Life Technologies	Customized
Recombinant DNA		
pCasSA	Addgene	98211
T2R14-Nanoluciferase	This study	N/A
GNAI2-Halo Tag	This study	N/A
GNAS-Halo Tag	This study	N/A
Gustducin-Halo Tag	This study	N/A
Software and algorithms		
Image Lab	Version 6.1	Bio-rad laboratories, Canada
Graph Pad Prism	Version 9.5.1	Graphpad.com
Soft Max Pro	Version 7.0	Molecular Devices

EXPERIMENTAL MODEL AND STUDY PARTICIPANT DETAILS

Cell lines and primary cells used in the study

BEAS-2B are transformed bronchial epithelial cells, which are widely utilized to investigate the functional properties of bronchial epithelial cells.[53] BEAS-2B cells were cultured using Bronchial Epithelial Cell Growth Medium (BEGM) consisting of Bronchial Epithelial Basal Medium with supplements, including 0.4% serum, and in plasticware with a collagen I coating to support and maintain the epithelial phenotype (see Lonza website for further info and references). The CHO-K1, NuLi-1 and CuFi-1 human airway cell line, homozygous for the ΔF508 mutation was purchased from ATCC. Primary bronchial epithelial cell lines employed in this study were sourced from the Primary Airway Cell Biobank at McGill University, Canada. The three CF primary cells (BCF: Female, 20 years; BCF: Male, 31 years and BCF: Male 44 years) used in this study are homozygous for F508del. Also, three non-CF primary cells (BD: Male, 59 years; BD: Female, 72 years and BD: Male, 50 years) were used as normal HBE. These were obtained under a materials transfer agreement (MTA). We observed similar expression pattern of T2R14 in all the BD (non-CF) and BCF (CF) donors via qPCR analysis. Therefore, we conducted T2R14 KD in one BD (non-CF HBE, BD: Male 59 years) and BCF (CF F508del/F508del, Female, 20 years) donor using short hairpin RNA (shRNA) approach through a lentiviral vector to knock down TAS2R14 in these HBEs and cultured them at the air-liquid interface (ALI).

HEK 293T cells stably overexpressing T2R14 was generated as described previously.[54]

Bacterial strains used in the study

The bacterial strains utilized were *Staphylococcus aureus ATCC 6538*, which is the wild type (WT), acquired from Dr. Duan's laboratory at the University of Manitoba. An *agrB* mutant strain of *Staphylococcus aureus*, denoted as *ΔagrB*, was created in our laboratory utilizing CRISPR-Cas9 technology (Figure S4 and supplementary methods). *Pseudomonas aeruginosa* strains included PAO1 (WT) and a LasI/R quorum sensing mutant designated as JP2 (*ΔlasI/ΔrhlI*), both of which were sourced from Dr. Duan's laboratory.

METHOD DETAILS

Co-culture assay on CF and non-CF HBE monolayer cells

For the co-culture assay, *S. aureus* ATCC 6538 (WT), *S. aureus ΔagrB, P. aeruginosa* PAO1[WT PAO1] and its Quorum Sensing Mutant *P. aeruginosa* JP2 strain were cultured overnight at 37°C with shaking at 200 rpm in the Luria-Bertani (LB) broth.

Infection assays were conducted using both CF (CuFi-1) and non-CF (BEAS-2B) bronchial epithelial cells cultured at monolayers. CuFi-1 and BEAS-2B cells ($1X10^6$) were plated in 6 well collagen type I coated plate with BEGM medium without any antibiotic for overnight and next day, cells were infected with either WT *S. aureus* or *S. aureus ΔagrB* at a multiplicity of infection (MOI) of 1:50 for 16-18 hours. Cell viability post-infection was assessed using the WST-1 assay.[50] Similarly, for *P. aeruginosa* infections, both CuFi-1 and BEAS-2B cells were treated with WT *PAO1* and the quorum sensing mutant *JP2* at an MOI of 1:10 for 4 - 6 hrs.[55] Following bacterial infections for appropriate period as mentioned above, cell culture supernatant was collected after filtration using 0.2-micron syringe filter and stored at -80°C for cytokine and HBD-2 analysis.

Generation of primary human airway epithelial airway-liquid interface (ALI) cultures

Human airway primary epithelial cells [both CF and non-CF] were grown in Explus medium. Upon reaching 80% confluency, cells were detached using 0.25% Trypsin-EDTA and seeded onto collagen-coated Transwell 24-well plates at a density of 500,000 cells/well.

Initially, both the apical and basolateral compartments were filled with 0.3 mL and 0.8 mL of Explus medium, respectively, and left for 2 days. Subsequently, the medium was replaced with Explus ALI medium from Lonza. The cultures were maintained until they achieved full confluency for 5–6 days, after which the basal medium was refreshed every other day until the 30th day. The establishment of ALI was verified by measuring Trans-epithelial Electrical Resistance (TEER) with values exceeding 500 $\Omega \cdot cm^2$ using a Voltohmmeter device from Millipore Sigma. After differentiation at ALI for 30 days, both CF and non-CF cells were visualized using Scanning Electron Microscopy (SEM)[56] (See Figures S1A and S1B).

Knockdown of T2R14 in CuFi-1, BEAS-2B and primary airway bronchial epithelial BD (non-CF) and BCF (CF) cells using shRNA lentiviral system

The *TAS2R14* gene, encoding for T2R14, was referenced using the standardized HUGO Gene Nomenclature Committee (HGNC) approved terms throughout this manuscript.[57] BEAS-2B and CuFi-1 cell lines with T2R14 knockdown (T2R14KD) were generated according to methodologies outlined in our previous studies.[11,58] Knock down of T2R14 mRNA transcript and protein was confirmed by qPCR and Western blot analysis, respectively, with antibody specificity detailed previously.[11] Similarly, the short hairpin RNA (shRNA) approach through a lentiviral vector was used to knock down TAS2R14 in both cystic fibrosis (BCF) and non cystic-fibrosis (BD) human bronchial epithelial cells cultured at the air-liquid interface (ALI), using an established protocol from the literature.[59]

Immunoblot analysis

Protein levels of Gαi, Gαs, PLCβ and Ggust proteins were quantified through immunoblotting. Cell lysates were prepared from control and T2R14 KD specific cells. Protein in the samples was estimated using Bio-Rad DC kit. Each sample, containing 20 μg of protein, was resolved on a 12% SDS-PAGE and subsequently transferred onto nitrocellulose membranes. These membranes were blocked using 5% non-fat dry milk for one hour at room temperature, followed by incubation with specific primary antibodies overnight at 4°C. The proteins were visualized by chemiluminescence, employing horseradish peroxidase (HRP)-conjugated secondary antibodies and enhanced chemiluminescence (ECL) substrate, with images captured using a ChemiDoc MP imaging system. Exposure times for chemiluminescence detection were set at 30 seconds for T2R14, and 5 seconds for the loading control, β-actin. Densitometric analysis of the bands was conducted utilizing Bio-Rad's Image Lab software.

NanoBRET

Plasmids for NanoBRET encoding Nanoluciferase and HaloTag were purchased from Promega Corp. Gene encoding human T2R14 (TAS2R14) was codon optimized and cloned into both these plasmids to obtain T2R14 with C-terminal tags. Genes encoding human Gαs (GNAS) and Gαi2 (*GNAI2*) were cloned into the parental plasmids to obtain each G protein with either N-terminal Nanoluciferase or HaloTag or C-terminal tag Nanoluciferase or HaloTag. Cloning was performed by Genscript and confirmed by sequencing. Plasmids were amplified by transformation into E. coli DH5α, and subsequent midi-prep using Qiagen columns. pcDNA3.1 was amplified for use as a carrier DNA.

Transfection: Calculated amounts of DNA (Nanoluciferase and HaloTag together, with or without carrier DNA) were diluted in OptiMEM at a concentration of 100 – 200 ng/μL. Lipofectamine 2000 was diluted in an equal volume of OptiMEM, such that 3 μL Lipofectamine was added for every 1 μg of DNA. The DNA solution was added to the Lipofectamine and allowed to form transfection complexes. These complexes were added to cells in solution, the suspension was mixed thoroughly and plated into 96-well plates, so that each well received 50,000 cells in 200 μL.

For testing the orientations of T2R14 and Gα subunits used in NanoBRET assays, cells were co-transfected with 1:10 ratio of Nanoluciferase : HaloTag plasmids, following the protocol as described above. At 24 hr post-transfection, the culture medium was replaced with 90 μL OptiMEM supplemented with 2% HI-FBS, and either Halo618 (100 μM stock solution in DMSO, final concentration 100 nM) or an equal volume of DMSO. Half the wells received Halo618 and the rest received DMSO treatment. After 12 hr the cells were centrifuged at 125xg for 2 minutes and treated with ligand. For ligand treatment, 20 mM DPH (10x) solution was prepared in OptiMEM, while control- buffer treatment used OptiMEM alone. Designated wells received 10 μL of DPH or buffer, were mixed for 30s on an oribital shaker at 120 rpm, and were incubated at 37°C for 5 minutes. At the end of this incubation, 25 μL of 5x NanoBRET NanoGlo substrate in OptiMEM was added to each well, and mixed on an orbital shaker as above. The reaction was incubated for 5 minutes at 23°C. Donor emission (luminescence) was measured at 460 nm and acceptor emission (Halo618 fluorescence) at 610 nm in a SpectraMax iD5 plate reader. Readings were converted to BRET ratio as follows

$$BRET\ ratio\ (milliBRET\ units) = \frac{Emission\ at\ 610\ nm}{Luminescence\ at\ 460\ nm} \times 1000$$

For donor saturation assays, DNA mixtures were prepared with 10 ng T2R14-Nanoluciferase plasmid, and 0.46 to 1000 ng of GNAI2-HaloTag plasmid, as described in the NanoBRET manual. The total DNA amount was kept constant by addition of pcDNA3.1. Transfection, Halo618 labeling, ligand treatment and BRET ratio calculation were performed as detailed above.

Intracellular calcium mobilization assay

Agonist induced intracellular calcium mobilization was assayed as described previously.[60] Both wild-type (WT), scrambled shRNA (sc ShRNA) and T2R14 knockdown (KD) NuLi-1, BEAS-2B and CuFi-1 cell lines, as well as primary non-cystic fibrosis (non-CF) and CF human bronchial epithelial (HBE) cells, were exposed to the following treatments: AIP-1 (50 μM) and increasing concentrations of DPH (31 μM -2000 μM), C12 (4.5 μM -300 μM), farnesol (7.5 μM -500 μM) or tyrosol (15 μM -1000 μM), Cells that had been seeded at a density of 25,000 per well in 96-well black-walled, clear-bottom plates pre-coated with type IV collagen (BD Optilux, VWR), were incubated for 16-18 hours. Subsequent exposures to DPH (different concentrations 31 μM -2000 μM), C12 (4.5 μM -300 μM), farnesol (7.5 μM -500 μM) or tyrosol (15 μM -1000 μM) and AIP-1 (50 μM), were used to investigate effects on T2R14. Intracellular calcium changes were quantified using a Flex Station® 3 MultiMode Microplate Reader, with data represented as the change in relative fluorescence units (RFU). Similarly, agonist induced intracellular calcium mobilization assays were performed in HEK293T cells overexpressing T2R14 as described previously after 3-oxo-12-AHL, C12 (4.5 μM -300 μM) and the fungal QSMs tyrosol (15 μM -1000 μM) and farnesol (7.5 μM - 500 μM) treatment.[11,60]

Determination of intracellular cAMP

Gαi-mediated cAMP accumulation was quantified using a Homogeneous Time-Resolved Fluorescence (HTRF)-based cAMP assay kit from CisBio, USA, following protocols described previously.[61,62] Briefly, 3000 cells/well were added in triplicate to wells in white 96-well plates (low volume white microplate, CisBio). To initiate inhibition via Gαi, cells were pre-treated with 3 μM forskolin, then exposed to 500 μM Diphenhydramine hydrochloride (DPH), 100 μM *P. aeruginosa* qsm C12, 50 μM *S. aureus* qsm AIP-1, or 100 μM *C. albicans* qsm tyrosol or farnesol. The detection range of the HTRF-based cAMP kit is 718,000 pM-150 pM. To inhibit Gαi activity, the specific peptide inhibitor, TAT-GPR (sequence: TMGEEDFFDLLAKSQSKRMDDQRVDLAK), was applied at 100 nM for 20 minutes, as suggested by the manufacturer and corroborated by prior studies.[63,64] 100 μM IBMX was included to inhibit cAMP degradation during the 30 min stimulation period, which was carried out on a plate shaker at room temperature. The HTRF signal was captured using a FlexStation® 3 Multi-Mode Microplate Reader (Molecular Devices, CA). FRET ratios (665/615 nm) were converted to cAMP concentrations using a standard curve according to the manufacturer's recommendations.

Measurement of nitrate/nitrite secretion

We measured the levels of nitrate/nitrite secreted from BEAS-2B, CuFi-1 (both wild-type and T2R14KD) grown in monolayer culture, and primary non-CF bronchial epithelial (BD) and CF human bronchial epithelial (BCF) cells cultured at the air-liquid interface (ALI). The cells were treated with 250 μM DPH, 100 μM C12, and 50 μM AIP-1 for approximately 16-18 hours. A 40 μL sample of the supernatant was then used for nitrate/nitrite quantification using a fluorescent assay kit (#780051, Cayman Chemical). The assay procedure involved mixing the reductase enzyme cofactor with the supernatant sample and incubating for 30 minutes at room temperature. This was followed by the addition of 2,3-diaminoapthelene (DAN) and sodium hydroxide (NaOH). The detection limit of the assay is 500–7.8 pmol. Fluorescence (excitation 365 nm, emission 460 nm) was measured using the FlexStation® 3 Multi-Mode Microplate Reader (Molecular devices, San Jose, CA, USA).

Human β-Defensin 2 (hBD-2) ELISA

BEAS-2B and CuFi-1 cells with and without T2R14KD were seeded in a 12-well plate at a density of 1.5 × 10^5cells/well. They were infected with *S. aureus* at a multiplicity of infection (MOI) of 50 for 18 hours and with *P. aeruginosa* at an MOI of 10 for 4-6 hours. Non-CF cells (BD) and CF (BCF) cells were cultured at the ALI and treated with 500 μM DPH, 100 μM C12, 50 μM AIP, 100 μM tyrosol or 100 μM farnesol for 18 hours. After treatment, the supernatant was collected and filtered through a 0.2 μm nylon filter and the filtrate used to quantitate the levels of secreted human β-defensin 2 (hBD-2), using ELISA (# 900-K172, PeproTech). The detection range of the assay is 1500–23 pg/mL. Absorbance at 450 nm (A_{450} nm) was measured by using the FlexStation® 3 (Molecular devices, San Jose, CA, USA).

Measurement of secreted cytokines (multiplexing) by eve technologies

BEAS-2B and CuFi-1 cells with and without T2R14 KD, were cultured in 12-well plates at a density of 1.5 × 10^5cells/well. These cells were then infected with *S. aureus* at a MOI of 50 for 18 hours and to *P. aeruginosa* at an MOI of 10 for 4-6 hours. BD and BCF cells at ALI were treated with DPH 500 μM, C12 100 μM, AIP 50 μM, farnesol 100 μM or tyrosol 100 μM each for 18 hrs. After the treatment, the supernatant was collected and filtered using a 0.2 μm nylon filter and used to quantify cytokine levels using multiplexing technology. The Luminex xMAP platform facilitated simultaneous measurement of 15 cytokines, chemokines, and growth factors, conducted by Eve Technologies (Calgary, Canada) utilizing the Luminex™ 200 system. Fifteen markers were measured simultaneously in the samples using Eve Technologies' Human Focused 15-Plex Discovery Assay® (MilliporeSigma, Burlington, Massachusetts, USA) according to the manufacturer's protocol. The 15-plex included: GM-CSF, IFNγ, IL-1β, IL-1Ra, IL-2, IL-4, IL-5, IL-6, IL-8, IL-10, IL-12p40, IL-12p70, IL-13, MCP-1 and TNF-α. Assay sensitivities for these markers range from 0.14 – 5.39 pg/mL. Individual analyte sensitivities values are available in the MilliporeSigma MILLIPLEX® MAP protocol.

Real time quantitative PCR (qPCR) method

qPCR analysis of ß2AR and *TAS2R14* gene expression in CF (BCF, n = 3) and non-CF (BD, n = 3) donors from the Primary Airway Cell Biobank at McGill University, and CF (CuFi-1) and non-CF (NuLi-1 and BEAS-2B) cell lines was performed. Total RNA was extracted, and cDNA were prepared from using the iscript cDNA synthesis kit (VWR, Canada). cDNA was then amplified using F and R primers for TAS2R14, ß2AR and GAPDH. The following protocol was used: 95°C/10 s, 39 cycles of 95°C/30 s, 60°C/30 s, 72°C/30 s, and a final extension at 72°C/1 min. In the qPCR quantification (Figure 1A), GAPDH was used as a housekeeping gene. The expression of both β2AR and TAS2R14 was normalized to GAPDH. The value of β2AR was next used to set the 100% level, and changes in TAS2R14 were compared to this level.

CRISPR protocol for the construction of the *agrBD* mutant of *S. aureus*, related to Figure S5

I. Insertion of spacers in the *BsaI* sites of the pCasSA plasmid Chen et al., 2017.[65]

II. Construction of the repair template

1. Digest 2μg pCasSA-XX-spacer plasmid with XbaI – XhoI by incubation with the enzymes and 1x CutSmart buffer (NEB) at 37°C for 2-3h. Heat inactivate at 65°C for 20min.
2. Purify the digested pCasSA-XX-spacer plasmid by using QIAquick Gel extraction kit as per the manufacturer's instructions.
3. To clone the repair templates into the *XbaI*/*XhoI* sites of the pCasSA-XX-spacer plasmid by Gibson assembly, the repair templates were prepared with the inclusion of the adaptor sequences (5' – TTTGAGATCTGTCCATACCCATG GTCTAGA – 3' attached at the 5' - end, and 5' -).
4. Insert the repair template into the *XbaI*/ *XhoI* sites of the pCasSA-XX-spacer plasmid by Gibson assembly using 10μL NEBuilder HiFi DNA Assembly Master Mix, 20fmol *XbaI*/ *XhoI* digested pCasSA-XX-spacer plasmid, 20fmol repair template and Milli-Q water to make volume up to 20μL.

Incubate at 50°C for 1h

5. Transform 5μL Gibson assembly product into DH5α competent cells. The colonies were selected on an LB agar plate containing 50μg/mL kanamycin. The success for the construction of the plasmid pCasSA-XX needs to be verified by PCR, enzyme digestion (*XbaI*/ *XhoI*).

All the primers used in the study are listed in Table S1.

III. Preparation of *S. aureus* electrocompetent cells

1. Pick an individual colony of the *S. aureus* strain and incubate it in 2mL TSB medium at 30°C overnight.
2. Dilute 1mL overnight culture into 100mL fresh TSB medium and shake it at 30°C until the optical density at 600 nm of the culture reached 0.3-0.4.
3. Chill the culture on ice for 10min.
4. Harvest the cells by centrifugation at 3000 x g for 5min at 4°C. Discard the supernatant.
5. Wash the cells with 20mL of sterile ice-cold 0.5M sucrose, twice.
6. Centrifuge again (3000 x g, 5min, 4°C). Discard the supernatant and re-suspend the cells with 1mL of 0.5M ice-cold sucrose.
7. Dispense the cells into 50μL aliquots in sterile tubes. Immerse the tubes into liquid nitrogen and store them at -80°C.

IV. Genome editing in *S. aureus*

1. Take a tube of the *S. aureus* competent cells and thaw it on ice for 5min.
2. Mix 1-2μg editing plasmid pCasSA-XX with the cells, and transfer the mixture into a 1mm electroporation cuvette.
3. Pulse the cells at Gene Pulser Xcell electroporation system. The parameters for electroporation were as follows: voltage 2100V, capacitance 100 ohm, and resistance 25μF.
4. After electroporation, immediately ad 1mL of TSB medium into the cuvette. Then transfer the cells into a 1.5mL sterile tube.
5. Shake the tube at 30°C for ∼1.5h.
6. Plate all the culture onto a TSB plate containing 30μg/mL chloramphenicol. Incubate the TSB plate at 30°C overnight.
7. Pick colonies from the plate and inoculate them individually into 3mL TSB medium containing 30μg/mL chloramphenicol. Incubate them at 30°C overnight.
8. Extract the genomic DNA using DNeasy Powersoil® Pro Kit as per the manufacturer's instructions.
9. Sequence the whole genome of the clone with Illumina i-seq100.

V. Plasmid Curing

1. Pick a colony of the confirmed *S. aureus* mutant that contains the pCasSA editing plasmid. Incubate it in TSB at 30°C overnight.
2. Dilute 3μL overnight culture into 3mL fresh TSB medium and incubate it at 42°C until the culture was evident.
3. Streak a fraction of the culture onto a TSB agar plate and incubate it at 37°C overnight.
4. Pick 4-6 individual colonies and incubate them in 3mL TSB overnight, individually.
5. Confirm the curing of the pCasSA plasmid by streaking a fraction of the culture onto TSB agar plates in the presence or absence of 50μg/mL chloramphenicol.

QUANTIFICATION AND STATISTICAL ANALYSIS

All experimental results are presented as the mean ± Standard error of the mean (SEM) from at least three independent experiments. GraphPad PRISM v9.0 (GraphPad Software, San Diego, CA, USA) was used to analyze statistical significance. One-way analysis of variance (ANOVA) was applied when comparing three or more groups. An unpaired two-tailed Student's t -test was used to compare two group data. Effect size computed as Hedges' *g* was compared by forest plot using the R package meta. Data are presented as mean ± standard error of mean (SEM); *p<0.05, **p<0.01, ***p<0.001, ****p<0.0001 as indicated. A Note on effect size and forest plots (to be read in relation to Figure 3D). In this work, effect size is the standardized mean difference calculated using Hedges' g statistic. First, we measured innate immune markers as secreted and calculated the mean value, in different conditions (± CF, and WT/KD of T2R14). The difference in means, divided by the standard deviation of the means yields the effect size. If there is a significant difference between the mean values of a marker (*t-test,* $p \leq 0.05$), then the effect size is displayed on the forest plot (Figure 3D). A positive shift in the effect size indicates a significantly larger response in the CF-conditions (whether T2R14 is WT or KD), while a negative shift in effect size indicates a lowered response in the CF condition, compared to the non-CF.